

Published in final edited form as:

Toxicol Appl Pharmacol. 2009 August 15; 239(1): 71–79. doi:10.1016/j.taap.2009.05.017.

N,N-Diethyldithiocarbamate promotes oxidative stress prior to myelin structural changes and increases myelin copper content

Olga M. Viquez^a, Barry Lai^b, Jae Hee Ahn^{a,†}, Mark D. Does^{c,d}, Holly L. Valentine^a, and William M. Valentine^{a,*}

^aDepartment of Pathology, Center in Molecular Toxicology and Center for Molecular Neuroscience, Vanderbilt University Medical Center, 1161 21st Ave. S., Nashville, TN 37232

^bAdvanced Photon Source Argonne National Laboratory, Argonne, IL 61439

^cDepartment of Biomedical Engineering, Vanderbilt University, Nashville, TN 37240

^dVanderbilt University Institute of Imaging Science, Vanderbilt University Medical Center, Nashville, TN 37232

Abstract

Dithiocarbamates are a commercially important class of compounds that can produce peripheral neuropathy in humans and experimental animals. Previous studies have supported a requirement for copper accumulation and enhanced lipid peroxidation in dithiocarbamate-mediated myelinopathy. The study presented here extends previous investigations in two areas. Firstly, although total copper levels have been shown to increase within nerve it has not been determined whether copper is increased within the myelin compartment, the primary site of lesion development. Therefore, the distribution of copper in sciatic nerve was characterized using synchrotron X-ray fluorescence microscopy to determine whether the neurotoxic dithiocarbamate, N,N-diethyldithiocarbamate, increases copper levels in myelin. Secondly, because lipid peroxidation is an ongoing process in normal nerve and the levels of lipid peroxidation products produced by dithiocarbamate exposure demonstrated an unusual cumulative dose response in previous studies the biological impact of dithiocarbamate-mediated lipid peroxidation was evaluated. Experiments were performed to determine whether dithiocarbamate-mediated lipid peroxidation products elicit an antioxidant response through measuring the protein expression levels of three enzymes, superoxide dismutase 1, heme oxygenase 1, and glutathione transferase a, that are linked to the antioxidant response element promoter. To establish the potential of oxidative injury to contribute to myelin injury the temporal relationship of the antioxidant response to myelin injury was determined. Myelin structure in peripheral nerve was assessed using multi-exponential transverse relaxation measurements (MET₂) as a function of exposure duration, and the temporal relationship of protein expression changes relative to the onset of changes in myelin integrity were determined. Initial assessments were also performed to explore the potential contribution of dithiocarbamate-mediated inhibition of proteasome function and inhibition of cuproenzyme activity to neurotoxicity, and also to assess the

© 2009 Elsevier Inc. All rights reserved

*Corresponding Author: Department of Pathology C3320 MCN VUMC Nashville, TN 37232-2561 e-mail bill.valentine@vanderbilt.edu fax 615-343-9825 phone 615-343-5836.

†Brentwood High School, Brentwood TN 37027

Publisher's Disclaimer: This is a PDF file of an unedited manuscript that has been accepted for publication. As a service to our customers we are providing this early version of the manuscript. The manuscript will undergo copyediting, typesetting, and review of the resulting proof before it is published in its final citable form. Please note that during the production process errors may be discovered which could affect the content, and all legal disclaimers that apply to the journal pertain.

Conflict of interest statement The authors declare that there are no conflicts of interest.

potential of dithiocarbamates to promote oxidative stress and injury within the central nervous system. These evaluations were performed using an established model for dithiocarbamate-mediated demyelination in the rat utilizing sciatic nerve, spinal cord and brain samples obtained from rats exposed to N,N-diethyldithiocarbamate (DEDIC) by intra-abdominal pumps for periods of 2, 4, and 8 weeks and from non exposed controls. The data supported the ability of DEDIC to increase copper within myelin and to enhance oxidative stress prior to structural changes detectable by MET₂. Evidence was also obtained that the excess copper produced by DEDIC in the central nervous system is redox active and promotes oxidative injury.

Introduction

Peripheral neuropathies have been observed in humans and produced in animals following administration of dithiocarbamates (Frisoni and Di Monda, 1989). In previous studies, oral administration of the acid stable dithiocarbamates pyrrolidine dithiocarbamate and disulfiram, or parenteral administration of the acid labile dithiocarbamate N,N-diethyldithiocarbamate (DEDIC), were shown to produce a primary myelinopathy in rats (Valentine *et al.*, 1998; Tonkin *et al.*, 2000; Tonkin *et al.*, 2003). In contrast, oral administration of DEDIC produced a CS₂-mediated neurofilamentous axonopathy resulting from in vivo acid promoted release of CS₂ (Johnson *et al.*, 1998). Based upon these findings it has been proposed that the parent dithiocarbamate is responsible for the observed myelin injury. In vitro systems have shown that the cytotoxicity of pyrrolidine dithiocarbamate in combination with copper is much greater than either copper or pyrrolidine dithiocarbamate alone (Chen *et al.*, 2000). The enhanced toxicity of the combination was ascribed to the ability of pyrrolidine dithiocarbamate to complex copper, transport it across the plasma membrane, and promote apoptosis through oxidative stress. Similarly, the redox activity of copper and accumulation of copper within the nervous system produced by certain dithiocarbamates has led to the hypothesis that myelinopathy producing dithiocarbamates form a lipophilic complex with copper that can cross the blood nerve barrier and promote lipid peroxidation leading to myelin injury. Experimental support for this hypothesis has been derived from in vitro models showing that dithiocarbamate complexes are redox active and that the ability of these complexes to produce lipid peroxidation is positively correlated to their lipophilicity (Nobel *et al.*, 1995; Valentine *et al.*, 2009). Correspondingly, an in vivo study showed that DEDIC but not sarcosine dithiocarbamate produced copper accumulation, oxidative stress with oxidative protein injury, and myelin lesions in peripheral nerve (Valentine *et al.*, 2009). This suggests that nonpolar nitrogen substituents are also required for dithiocarbamate-mediated copper accumulation in the nervous system and the development of a myelinopathy.

If dithiocarbamate-copper complexes are responsible for lipid peroxidation induced myelin injury, then it would be expected that the levels of copper within myelin would be elevated and that the increase in lipid peroxidation products previously reported (Viquez *et al.*, 2008) would be sufficient to evoke an antioxidant response prior to myelin injury. In the study presented here the distribution of copper and seven other elements in sciatic nerve were characterized using synchrotron X-ray fluorescence microscopy (micro-XRF) to determine whether copper levels are altered within myelin in dithiocarbamate-induced myelinopathy. To ascertain whether the previously reported elevations in lipid peroxidation products are accompanied by a cellular antioxidant response the protein expression levels of three enzymes, superoxide dismutase 1 (SOD-1), heme oxygenase 1 (HO-1), and glutathione transferase α (GST- α), that are linked to the antioxidant response element were quantified as a function of dithiocarbamate exposure duration. An initial evaluation of the potential of dithiocarbamates to inhibit cuproenzyme activity in vivo was also performed through measuring the activity of SOD-1. Myelin composition of peripheral nerve was also assessed using multi-exponential transverse relaxation (MET₂) analysis as a function of exposure duration, and the temporal

relationship of protein expression changes relative to the onset of changes in myelin integrity, as assessed by MET₂, were determined. Initial assessments were also performed to explore the potential contribution of dithiocarbamate-mediated inhibition of proteasome function to neurotoxicity, and also to assess the potential of dithiocarbamates to promote oxidative stress and injury within the central nervous system. These evaluations were performed using an established model for dithiocarbamate-mediated demyelination in the rat examining sciatic nerve, spinal cord and brain samples obtained from rats exposed to N,N-diethyldithiocarbamate (DEDC) by intra-abdominal pumps for periods of 2, 4, and 8 weeks and from non exposed controls.

Materials and methods

Chemicals

2ML4 Alzet® osmotic pumps were obtained from Braintree Scientific (Braintree, MA). Sodium N,N-diethyldithiocarbamate (DEDC) and sodium cyanoborohydride (NaCNBH₃) were obtained from Alfa Aesar (Ward Hill, MA). Fluoresceinamine (5-aminofluorescein) was purchased from Tokyo Chemical Industry (TCI) America (Portland, OR). Protease and phosphatase inhibitors were purchased from Amersham Biosciences (Piscataway, NJ) and Sigma-Aldrich (Saint Louis, MO). Bovine serum albumin (BSA), HEPES, MgCl₂ and KCl were obtained from Sigma-Aldrich (St. Louis, MO). Dulbecco's PBS (pH 7.4) was purchased from MP Biomedicals (Irvine, CA). All HPLC grade solvents were purchased from Fisher Scientific (Pittsburgh, PA).

Animals and exposures

All treatments and procedures using animals were conducted in accordance with the National Institutes of Health *Guide for Care and Use of Laboratory Animals* and approved by the Institutional Animal Care and Use Committee of Vanderbilt University. Twenty-seven adult male Sprague-Dawley rats were obtained from Harlan Bioproducts (Indianapolis, IN) and caged at Vanderbilt University animal facilities in a temperature controlled room (21-22 °C) with a 12 h light-dark cycle, supplied with Purina Lab Diet 5001, a segment of 4 inch diameter PVC tubing for environmental enrichment and water *ad libitum*. After a 10-14 day acclimatization period, animals were assigned to either a control or exposure group of 2, 4 or 8 weeks, *n* = 4 per group, except for the 8-week time point where *n* = 5 (control) and *n* = 6 (DEDC-exposed). For the exposure groups DEDC was administered at 0.3 mmol/kg/day using intra-abdominal 2mL 4-week Alzet® osmotic pumps (Braintree Scientific, Braintree, MA) surgically implanted under anesthesia (100 mg/Kg ketamine with 8 mg/Kg xylazine ip). The osmotic pumps were replaced after 4 weeks to extend the exposure period to 8 weeks. Sham pump implantation surgery was not performed on control animals. The average starting body weight of all 27 animals was 318.4 ± 1.7 g (SE), and all animals were weighed twice a week during the experiment.

At the end of each exposure period, control and exposed animals were deeply anesthetized with pentobarbital (100 mg/Kg body weight, i.p.). The animals were then perfused through the left ventricle of the heart with PBS (pH 7.4) and tissues collected. The left sciatic nerve, half of the brain cut sagittally, and sections of thoracic proximal spinal cord were removed and immediately frozen in liquid nitrogen and stored at -80 °C for protein expression analysis, carbonyl content, proteasome and SOD activities. The right sciatic nerve was immersed in 4% glutaraldehyde in 0.1 M PBS (pH 7.4) and stored at 4°C for MET₂. Portions of nerves used for micro-XRF were also postfixed in osmium tetroxide and embedded in Spurr.

Synchrotron X-ray Fluorescence Microscopy (micro-XRF)

Scanning X-ray fluorescence microscopy was performed at the 2-ID-D beamline of the Advanced Photon Source at Argonne National Laboratory (IL, USA) (Cai *et al.*, 2000). The source was a 3.3-cm-period undulator, and x-rays were monochromatized by a double-crystal Si(111) monochromator. A Fresnel zone plate focused the x-ray beam on the sample to a spot size of 0.3 (h) × 0.2 (v) μm^2 (Yun *et al.*, 1999). The flux at the focal spot was measured to be $\approx 4 \times 10^9$ photons/sec using an ionization chamber in place of the sample. The specimen was placed in a helium environment and mounted on a X-Y translation stage at 75° to the incident beam. An energy-dispersive silicon drift detector (SII NanoTechnology) was used to collect x-ray fluorescence spectra from the sample while it was being scanned across the focus spot. In this way, spatial maps of many different elements were acquired simultaneously. An incident x-ray energy of 10 keV was used to excite K_{α} emission lines for elements from Si to Zn. At this energy x-rays penetrate biological specimens without significant absorption nor beam spreading; thus no specimen thinning is required and fluorescence maps of individual elements represent a 2D projection of the volumetric distribution within the specimen

The specimen (1 mm thick section of nerve) supported on a thin silicon nitride membrane was placed onto a kinematic specimen holder suitable for both optical and X-ray fluorescence microscopy. The specimen was first examined under a visible light microscope (Leica DMXRE) and selected areas of interest were located relative to reference points of the silicon nitride membrane using a high resolution motorized x/y stage (Ludl Bioprecision). Coordinates were recorded and were used to precisely locate the target area once the specimen was transferred to the x-ray microprobe.

Spectral Analysis

Using the program MAPS (Vogt, 2003), the spectrum at each pixel was individually fitted to remove overlaps between adjacent K_{α} emission lines in order to achieve more accurate quantification. Elemental fluorescence intensities were converted to areal densities in $\mu\text{g}/\text{cm}^2$ by comparing x-ray fluorescence intensities with those from thin film standards NBS-1832 and NBS-1833 (NIST, Gaithersburg, MD).

Sciatic nerve multi-exponential transverse relaxation (MET_2) measurements

One glutaraldehyde-fixed sciatic nerve (≈ 10 mm) from each animal was placed into a 5mm (o.d.) NMR tube. The tube was filled with perfluorocarbon solution (fomblin) to prevent tissue drying without contributing proton signal; and the nerve was held below the fluid surface with a teflon plug. NMR data were acquired at 300 MHz, at room temperature (≈ 20 °C), using a 16-cm bore 7T horizontal MRI system with a home-built, 10-mm diameter loop gap resonator. For each sample, a Carr Purcell Meiboom Gill (CPMG) pulse sequence using ≈ 20 μs refocusing pulses, 1-ms echo spacing, 1000 echoes and a 15 s pre-delay was used to acquire data. From these data, even echo magnitudes were extracted and T_2 spectra were computed by fitting a sum of 200 decaying exponential functions with time constants logarithmically distributed between 2 ms and 2 s and smoothed with a minimum energy constraint (Whittall and MacKay, 1989). The spectra generally exhibited three distinct T_2 components, consistent with the aforementioned studies. The domains of these spectral components were defined as 10-40 ms, 40-150 ms, and >150 ms. The sum of total signal over each range was divided by the sum of signal of all the ranges for each spectrum to give the percent of total area for each T_2 component.

Western blotting for GST- α , HO-1 and SOD-1

Approximately 10 mg of frozen sciatic nerve or 150 mg of frozen brain was powdered in a mortar and pestle in liquid nitrogen. Spinal cord proteins were extracted from ≈ 40 mg of frozen tissue by sonication (Sonic Dismembrator Model 60, Fisher Scientific) followed by extraction

using 0.2 - 0.6 mL chilled TNE buffer (2 mM EDTA, 150 mM NaCl, 50 mM Tris-base, 2 mM DTT, and NP-40 (1%, v/v)), containing protease inhibitors (P-2714 Sigma-Aldrich, St. Louis, MO, one vial dissolved in 10mL water and added to the extraction buffer at 1%, v/v and 80-6501-23 protease inhibitor mix, Amersham Biosciences, Piscataway, NJ, 1%, v/v) and phosphatase inhibitors (P-2850 and P-5726 Sigma-Aldrich 1%, v/v). The homogenate was sonicated in an ice/water bath for 3 min and centrifuged at 40,485×g for 20 min at 4 °C. The supernatant was collected and stored at -80 °C. Protein concentration in the supernatant of the tissue samples was measured by a modified Bradford method (Ramagli, 1999) using BSA as the standard.

Equal amounts (10-25 µg) of sciatic nerve, spinal cord or brain protein were separated by SDS-PAGE (NuPAGE® 4-12% bis-tris gel, Invitrogen, Carlsbad, CA) along with molecular weight markers (Novex®Sharp Pre-Stained Protein Standards (MW 3.5-260 kDa), MagicMark™XP Western Standard, Invitrogen Carlsbad, CA). Separated proteins were electrophoretically transferred onto an Immobilon-P membrane using an XCell II™ Blot Module (Invitrogen, Carlsbad, CA). Nonspecific binding sites were blocked in blocking buffer (5% nonfat powdered skim milk in tris buffered saline, pH 7.4, containing 0.1% Tween-20 (TBST)) at room temperature for 1 h. Membranes were then incubated with primary antibodies against GST-α (GSTA11: rabbit anti-GST-α, Alpha Diagnostic, San Antonio, TX, dilution 1:2,000) or SOD-1 (FL-154: sc-11407, Santa Cruz Biotechnology, Santa Cruz, CA, dilution 1:5,000) or HO-1 (OSA-111, Stressgen, Ann Arbor, MI, dilution 1:2,500) overnight at 4 °C.

Concurrently, with the above primary antibodies, membranes were also incubated with primary anti-actin antibody (A-2066, rabbit anti-actin, Sigma, St. Louis, MO, dilution 1:5,000). After rinsing with TBST, the membranes were incubated at room temperature for 1hr with anti-rabbit peroxidase conjugated secondary antibody (A-8275, Sigma, St. Louis, MO, dilution 1:10,000). Following three 10 min washes in TBST, the membranes were incubated with Western Lightning Chemiluminescence Reagent Plus substrate (Perkin-Elmer LAS, Inc., Boston, MA), and exposed to Kodak X-Omat Blue XB-1 film. The presence of GST-α (MW ≈ 25 kDa) and SOD-1 (MW ≈ kDa) was confirmed by comparing the migration of positive control GST (rat liver, Sigma, St. Louis, MO) or SOD-1 (bovine liver, Alexis Biochemicals, San Diego, CA) to the molecular weight standard. The presence of actin (MW≈ 42 kDa) and HO-1 (MW ≈ 32 kDa) were confirmed by comparison to the molecular weight standard. For quantification, films were scanned with a GS-700 densitometer (Bio-Rad, Hercules, CA) and analyzed using Quantity One 1-D Analysis Program version 4.1 (Bio-Rad). Normalization of gel proteins loads was performed for each sample relative to actin.

Carbonyl determination

The protein carbonyl content of samples and standards was determined by the fluoresceinamine-cyanoborohydride method using immunochemical detection as previously described (Levine *et al.*, 1990). Briefly, 25 µg aliquots of protein were treated with fluoresceinamine (12 µL of 0.25 M) and sodium cyanoborohydride (10 µL of 0.4 M) for 1 hr at 37°C. Next, protein was precipitated at room temperature with ethanol:water:chloroform (4:3:1, v/v). Precipitates were washed 5 times with acidified ethanol:ethyl acetate (1:1) for 5 min at 37°C followed by centrifugation (13,000 rpm, 10 min) and then solubilized in 250 µL sodium hydroxide (0.1 N) for 15 min at 37°C. Treated proteins (controls or DEDC exposed) were bound to Immobilon-P membranes (Millipore, MA) using the Bio-Slot® Blot apparatus (BioRad, Hercules, CA). Four replicates per sample containing approximately 0.25 µg of sciatic nerve protein per well were loaded. Protein carbonyls were detected using the CDP-Star Universal Alkaline Phosphatase kit (Sigma-Aldrich Co., St. Louis, MO) following the manufacturer's instructions. Kodak X-Omat Blue XB-1 film was exposed to the treated membrane at room temperature for 50 min. For quantification, films were scanned with a GS-700 densitometer and analyzed using Quantity One® 1-D Analysis Program version 4.1

(Bio-Rad, Hercules, CA). The protein carbonyl content of samples was determined from a standard curve generated using oxidized BSA for which carbonyl content was determined spectrophotometrically ($\epsilon=86,000 \text{ M}^{-1}\text{cm}^{-1}$ at 490 nm) using a Shimadzu UV-2401 PC. Oxidized BSA standards were prepared by incubating 10 mg of BSA dissolved in 1 ml of 20 mM TrisHCl (pH 7.4) with 100 mM Fe^{2+} and 100 mM hydrogen peroxide, at room temperature for 1 hour. Reduced BSA was prepared by mixing oxidized-BSA (10 mg/mL) with 5 mg of sodium borohydride for 30 min at 37°C. The quantity of protein bound to the PVDF membrane was determined using the MemCode™ Reversible Protein Stain Kit for PVDF membranes (Pierce, Rockford, IL) using BSA as standards.

Preparation of biological samples for proteasome and SOD activities

Frozen sciatic nerve, spinal cord or brain tissue was powdered in a mortar and pestle in liquid nitrogen, and homogenized in 0.2 mL of cold HEPES buffer (10mM HEPES (pH = 7.9); 1.5mM MgCl_2 ; 10mM KCl). The homogenate was sonicated in an ice/water bath for 3 min and centrifuged at 40,485×g for 20 min at 4 °C. Half of the supernatant was collected, aliquoted, stored at -80 °C, and then used to measure proteasome activity. The remaining supernatant was extracted with ethanol/chloroform to inactivate Mn-SOD. Briefly, ice-cooled ethanol/chloroform (62.5/37.5 (v/v) was added to the supernatant and vortexed for 30 seconds, and then centrifuged at 5,000×g for 5min at 4 °C. The upper aqueous layer or cytosolic fraction was collected, and immediately used to measure SOD activity. Protein concentration in the supernatant of the tissue homogenate and the cytosolic fraction was measured using a modified Bradford method (Ramagli, 1999) with BSA as the standard.

Analysis of CuZn superoxide dismutase (SOD-1) activity

The SOD-1 activity was measured in sciatic nerve, spinal cord and brain extracts using the BIOXYTECH® SOD-525™ Assay (Oxis International, Inc., Foster City, CA). This assay is based on the SOD-mediated increase in the rate of autoxidation of 5,6,6a,11b-tetrahydro-3,9,10 trihydroxybenzo[c]fluorene in aqueous alkaline solution, yielding a chromophore with maximum absorbance at 525 nm. All assays were performed following the manufacturer's direction except that the reaction was performed at 25 °C, following buffer equilibration at the same temperature. Briefly, 40 mL of cytosolic fraction freshly prepared as described above or water was added to 900 μL of equilibrated buffer, and then 30 mL of 1-methyl-2-vinylpyridinium was then added, thoroughly vortexed and incubated for 1 min at 25 °C. To each reaction 30 mL of 5,6,6a,11b-tetrahydro-3,9,10 trihydroxybenzo[c]fluorene was added and the change in the absorbance at 525 nm was immediately monitored for 10 minutes. The SOD activity [units] of each sample was calculated from the maximum slopes of the sample (V_s) and blanks (V_c , obtained from the average of 4-6 blanks) using the following equation $[\text{SOD}] = 0.93 * ((V_s - V_c) / V_c) / (1.073 - 0.073 * (V_s / V_c))$. Specific activity of SOD was reported as units/mg protein.

Assay of proteasome activity

Quantification of proteasome activity in sciatic nerve, spinal cord or brain supernatants was determined using the 20S proteasome Fluorometric (AMC) assay Kit from CHEMICON International (Temecula, CA). This assay measures the fluorophore 7-amino-4-methylcoumarin (AMC) released from the LLVY-AMC substrate by proteasomal cleavage. Free AMC fluorescence was quantified using a SpectraMax M5 / M5° Microplate Reader using 380/460 nm filter set. Supernatant of sciatic nerve, brain or spinal cord extracts were added to the assay mixture following the manufacturer's specifications and incubated for 1 hr at 44 °C with the proteasome substrate. Proteasome activity was calculated from a standard curve generated using an AMC standard and reported as μM of AMC/mg protein.

Statistical Analysis

One-way analysis of variance (ANOVA), unpaired one-tailed and two-tailed student's t-tests, Tukey-Kramer's Multiple Comparisons Test, Dunnett's multiple comparison post hoc test and the Pearson Correlation test were performed using InStat 3.0 (Graphpad Software, Inc.). Statistical significance was taken to be $p < 0.05$ unless otherwise noted.

Results

Synchrotron X-ray Fluorescence Microscopy

Comparisons of total element levels demonstrated a significant increase of Cu in DEDC exposed nerves relative to controls (Table 1). No significant differences in total levels were detected for any of the other elements; however, small differences may not have been detected due to the power associated with the sample size used. Most elements were localized to the myelin, axoplasm, or endoneurial compartments in the two-dimensional element maps (Figure 1). The highest concentrations of Cu, S, P and K were localized to myelin whereas Cl was most concentrated within the axoplasm for both exposure groups. In contrast the distributions of Ca and Zn within the nerves appeared different for the exposed animals relative to control animals. In the two-dimensional maps for control nerves the highest concentrations of Ca and Zn were in the endoneurium; whereas, both Ca and Zn were more concentrated within myelin in the DEDC exposed nerves. Segmentation of the images into a myelin compartment and an axoplasm combined with endoneurium compartment (Figure 2A) and quantification of Zn and Ca in each compartment demonstrated a significant increase in the ratio of the mean myelin concentration relative to axoplasm and endoneurium compartment for both Zn and Ca. Statistical comparisons of the individual compartments showed there was a significant decrease of Zn and Ca in the combined endoneurium and axoplasm compartment (Figure 2B). Similar quantitative comparisons for Cu demonstrated that copper was significantly elevated in the myelin compartment as well as in the axoplasm and endoneurial compartment.

MET₂ spectra analysis

Representative T₂ relaxation spectra for fixed sciatic nerves obtained from a control and a 4 week DEDC exposed rat are shown in Figure 3A illustrating the short, intermediate, and long T₂ water components. The overlays of the T₂ spectra of the treated and control nerves show a decrease in the contribution of the shortest T₂ component to the total peak area for the exposed nerve relative to the control. Changes in the three water T₂ components as a function of exposure duration are presented in Figure 3B. Significant correlations to exposure duration were observed for all three components area contributions with the short and long T₂ water components exhibiting a negative correlation ($p < 0.05$ with $r^2 = 0.89$ and $p < 0.05$ with $r^2 = 0.87$, respectively) and the intermediate T₂ component a positive correlation ($p < 0.01$ with $r^2 = 0.98$). The ratios of the percent contribution to total peak area for the long component/short component, intermediate component/short component and the intermediate component/(short + long) components as a function of exposure duration are shown in Figure 3C. Significant increases were observed at the 4 and 8 week exposure time points for the intermediate component/short component and the intermediate component/(short + long) components ratios relative to those for controls.

Protein expression levels of SOD-1, HO-1 and GST- α

Western blots of sciatic nerve and spinal cord proteins showed significant increases in the levels of antioxidant enzymes (Figure 4). In nerve, SOD-1 was elevated at the 8 week time point, HO-1 at 4 and 8 weeks, and GST- α at 2, 4 and 8 weeks of DEDC exposure. In spinal cord elevations of SOD-1 were detectable at 4 and 8 weeks and significant elevations of HO-1 and GST- α were observed at 2, 4 and 8 weeks. Significant positive correlations to duration of

exposure were observed for GST- α in the spinal cord ($p < 0.01$ $r^2 = 0.98$) and nerve ($P < 0.01$ $r^2 = 0.99$) samples and for SOD-1 in nerve ($p < 0.05$ $r^2 = 0.92$).

Protein carbonyl content

Slot-blot and subsequent immunochemical detection of fluoresceinamine derivatized protein carbonyls demonstrated a significant increase in the protein carbonyl content of nerve and spinal cord proteins isolated from rats exposed to DEDC relative to that of controls (Figure 5). In nerves, significant increases were observed at all time points examined; and in spinal cord, a significant increase was detected at 8 weeks of exposure.

SOD-1 and proteasome activity

The levels of SOD-1 activity determined from the rate of autoxidation of 5,6,6a,11b-tetrahydro-3,9,10 trihydroxybenzo[c]fluorine in brain, spinal cord and sciatic nerve extracts were all significantly elevated in DEDC exposed animals relative to controls (Figure 6A). There were no significant differences in brain, spinal cord, or nerve proteasome activity between DEDC exposed and control samples as determined by cleavage of the LLVY-AMC substrate (Figure 6B).

Discussion

X-ray fluorescence spectrometry induced by synchrotron radiation is a nondestructive analytical method that provides topographical and quantitative elemental analysis of samples (Paunesku *et al.*, 2006; Fahrni, 2007). Previous studies have used this methodology to localize metals within dopaminergic neurons in vitro and spinal cord sections obtained from amyotrophic lateral sclerosis patients (Chwiej *et al.*, 2005; Carmona *et al.*, 2008). The two-dimensional elemental maps generated here for peripheral nerve provided considerable structural detail of myelinated axons for most of the elements examined, with myelin, endoneurial and axoplasmic compartments easily discernable. The highest concentrations of Cu were located within myelin for DEDC exposed and control groups. Myelin basic protein and P0, which are integral structural proteins of compact myelin, have been shown to bind Cu with high affinity and may have contributed to the observed localization of Cu to myelin (Sedzik *et al.*, 1999; Sabour *et al.*, 2002). Similarly, the relatively high phospholipid content of myelin could account for the greater concentration of phosphorous in myelin for both exposure groups. Interestingly, in the two-dimensional elemental maps the controls appeared to have the greatest concentrations of Zn and Ca within the endoneurium whereas in DEDC exposed rats these elements appeared more concentrated in myelin. The calculated ratios of myelin/(endoneurium and axoplasm) concentrations for Zn and Ca supported this interpretation as well. However, based upon the comparisons of mean element concentrations in like compartments for each treatment group the shift in the relative concentration of Zn and Ca for myelin did not result from changes within myelin itself, but rather from a decrease in the endoneurial content. Although a previous study observed a decrease for Zn in nerve from dithiocarbamate exposure this has not been a consistently reported finding (Tonkin *et al.*, 2004; Calviello *et al.*, 2005). However, the analytical methods used in previous studies did not provide information on the distribution of elements within nerve and the data derived here from micro-XRF suggests that although total levels may not be significantly changed, the distribution of Ca and Zn within nerve is altered. Whether this change in distribution was a primary effect of DEDC and contributes to the development of myelin lesions or a consequence of myelin injury will require further investigation.

Consistent with previous studies measuring total copper using ICP/MS or AAS (Tonkin *et al.*, 2004; Calviello *et al.*, 2005), the analyses of nerve by micro-XRF detected a significant increase in total copper for the nerves obtained from DEDC exposed rats relative to controls.

However, the 2-dimensional elemental maps obtained using micro-XRF provided new information on the distribution of the excess copper in nerve. Previous studies have supported the requirement for the generation of a nonpolar copper complex by dithiocarbamates to impart neurotoxicity and this property appears to determine the ability of a dithiocarbamate to elevate copper levels within the nervous system (Valentine *et al.*, 2009). Production of a primary myelin injury through copper mediated lipid peroxidation also suggests a requirement that copper levels be elevated within myelin. The data obtained using micro-XRF analysis demonstrated that copper was significantly elevated within the myelin of the sections prepared from DEDC exposed rats relative to controls. Comparisons of the compartmental levels of copper did not support a preferential accumulation of copper in myelin but were more consistent with a uniform increase of copper in all the compartments within nerve. Given this uniform increase of copper it is not clear why myelin is the primary site of lesion development. Two possibilities are that myelin is the most sensitive target for the excess copper, possibly due to myelin's high content of polyunsaturated fatty acids, or that the copper present within the myelin is in a more biologically active form. Further studies determining the oxidation state and chemical species of the excess copper within myelin and other nerve compartments using X-ray absorption near-edge structure spectroscopy and complimentary analytical methods will aid in understanding the apparent greater sensitivity of myelin.

Transverse relaxation of proton magnetization in peripheral nerve is multi-exponential and contains at least three components (Vasilescu *et al.*, 1978). Previous studies have interpreted these individual components to represent populations of water protons in nerve that undergo slow exchange on the magnetic resonance time scale. A consistent finding in previous studies using MET₂ to evaluate crush and demyelinating injury in peripheral nerve has been a decrease in the relative contribution of the short T₂ component to total MET₂ spectrum (Does and Snyder, 1996; Bendszus *et al.*, 2004). This decrease has been interpreted and supported by morphology assessments to correspond to a decrease in the total myelin content within nerve (Webb *et al.*, 2003). Assignment of the intermediate- and long-lived T₂ components is less clear. However, the current prevailing interpretation presented by Vasilescu is that the intermediate- and long-lived components are derived, respectively, from axoplasm and extra-cellular water, and this interpretation was supported by at least two later studies (Menon *et al.*, 1992; Beaulieu *et al.*, 1998). Consequently, we interpret the observed decrease in the contribution of the shortest T₂ component with continued DEDC exposure to reflect an overall loss of compact myelin or change in its structural integrity. Additionally, the observed increases in the intermediate component's contribution suggests an increase in axoplasm water relative to both myelin and extra-axonal water.

The ratio derived from the areas of the axoplasm and myelin T₂ components is analogous to the axon g ratio (axon diameter/total fiber diameter, i.e., axon with myelin) that is a commonly used parameter for assessing the morphology of myelinated axons. The g ratio provides an index of changes in the myelin content of nerve relative to that of axons (King, 1999) with increases in the g ratio resulting from thinning or loss of myelin. It is interesting to note that a significant increase in the ratio of the intermediate/short components was detected at shorter exposure durations than those required for the development of lesions detected by light microscopy (Viquez *et al.*, 2008) supporting the potential of MET₂ analysis for evaluating subtle changes in myelin.

Previous studies have demonstrated that DEDC administration is accompanied by elevations in lipid peroxidation products and protein levels of antioxidant enzymes in peripheral nerve (Viquez *et al.*, lesions and is not a nonspecific sequelae to inflammation accompanying the myelin injury has been provided by the observation that lipid peroxidation is increased after 2 weeks of exposure whereas lesions and activated macrophages were not detectable by light microscopy until 8 weeks of exposure (Viquez, *et al.*, 2008). Interestingly, the levels of lipid

peroxidation products in that study appeared to peak early during the course of exposure and then decrease in magnitude at subsequent time points examined. To further define the temporal relationship of oxidative stress and injury to the onset of myelin structural changes in dithiocarbamate-mediated myelinopathy, three proteins, SOD-1, HO-1 and GST- α , in conjunction with protein carbonyl levels were determined as a function of exposure duration at periods shorter and equal to that determined to produce myelin structural injury by DEDC. These assessments were also performed on spinal cord samples to examine the biological response of the CNS. These three proteins are regulated, at least in part, by the binding of the NF-E2 p45-related factor (Nrf2) to the antioxidant response element and typically exhibit increased expression levels under conditions of increased oxidative stress (Nguyen *et al.*, 2003). The fluoresceineamine assay used here reflects the generation of aldehyde moieties on proteins from metal-catalyzed oxidation of prolyl, lysyl, and arginyl residue side chains and from the addition of reactive lipid peroxidation products to protein nucleophilic sites and thus reflects oxidative protein injury (Levine *et al.*, 1990). In nerve, significant elevations in protein carbonyls and protein levels of GST- α were observed at the earliest time point, 2 weeks. This suggests that the previously reported increases of lipid peroxidation products prior to myelin injury are adequate to invoke an antioxidant response and produce oxidative injury. Additionally, because GST- α and other isoforms of GST are important in detoxifying reactive lipid peroxidation products and have peroxidase activity for the reduction of phospholipid peroxides (Awasthi *et al.*, 2005), the elevated expression of GST- α with continued exposure may partially account for the corresponding decreases in malondialdehyde and F₂-isoprostanes at later time points (Viquez *et al.*, 2008). DEDC also significantly increased expression of antioxidant enzymes in the spinal cord as early as 2 weeks for HO-1 and GST- α suggesting that the elevations in copper produced by DEDC in spinal cord have analogous biological effects to those produced in peripheral nerve.

The ubiquitin-proteasome system is important in the turn over of proteins and preventing the accumulation of damaged and misfolded proteins. Inhibition of proteasome activity can induce apoptosis, and abnormal proteasome function is thought to contribute to several neurodegenerative diseases through compromised removal of oxidatively damaged and misfolded proteins (Rubinsztein, 2006). Because proteasome inhibition can induce apoptosis, and proliferating cancer cells are more sensitive to proteasome inhibitors than normal or untransformed cells, proteasome inhibitors, including some dithiocarbamates, are currently being explored as chemotherapeutic agents (Daniel *et al.*, 2005; Chen *et al.*, 2006; Yu *et al.*, 2007). In the current study 26S proteasome activity was measured in sciatic nerve, spinal cord and brain samples as an initial evaluation of the ability of DEDC to inhibit proteasome function in vivo. The data obtained was consistent with no significant inhibition of proteasome function within the peripheral or central nervous systems; however, because only chymotrypsin-like activity was measured, dithiocarbamate-mediated effects on other activities essential to proteasome activity cannot be ruled out. Inhibition of SOD-1 due to sequestering of the required copper cofactor could contribute to the oxidative stress observed in DEDC myelinopathy. However, in contrast to a previous study that measured decreased SOD-1 activity in mice after a single dose (Heikkila *et al.*, 1976), in the present study SOD-1 activity increased in sciatic nerve, spinal cord and brain in DEDC exposed animals from repeated dosing. Since SOD-1 protein levels were also increased in the DEDC exposed samples the results suggest that SOD-1 was not significantly inhibited under the exposure conditions used in the present study that produced a myelinopathy.

The experiments in the study reported here support the ability of DEDC to increase copper within myelin and to enhance oxidative stress in nerve prior to structural changes detectable by MET₂. Evidence was also obtained that the excess copper produced by DEDC in the central nervous system is redox active and enhances oxidative stress. Because previous studies have shown that the relative increase in copper for the central nervous system is much greater than

that in peripheral nerve following DEDC exposure further investigation on the biological effects of dithiocarbamates in the central nervous system appears warranted. Also, because copper and the abnormal expression and aggregation of several copper binding proteins are involved in prominent neurodegenerative diseases (Brewer, 2008; Desai and Kaler, 2008), delineating the biological effects of dithiocarbamates and elevated copper within the central nervous system will provide insight regarding the potential of these widespread environmental compounds to modulate neurodegenerative diseases through copper dysregulation.

Acknowledgements

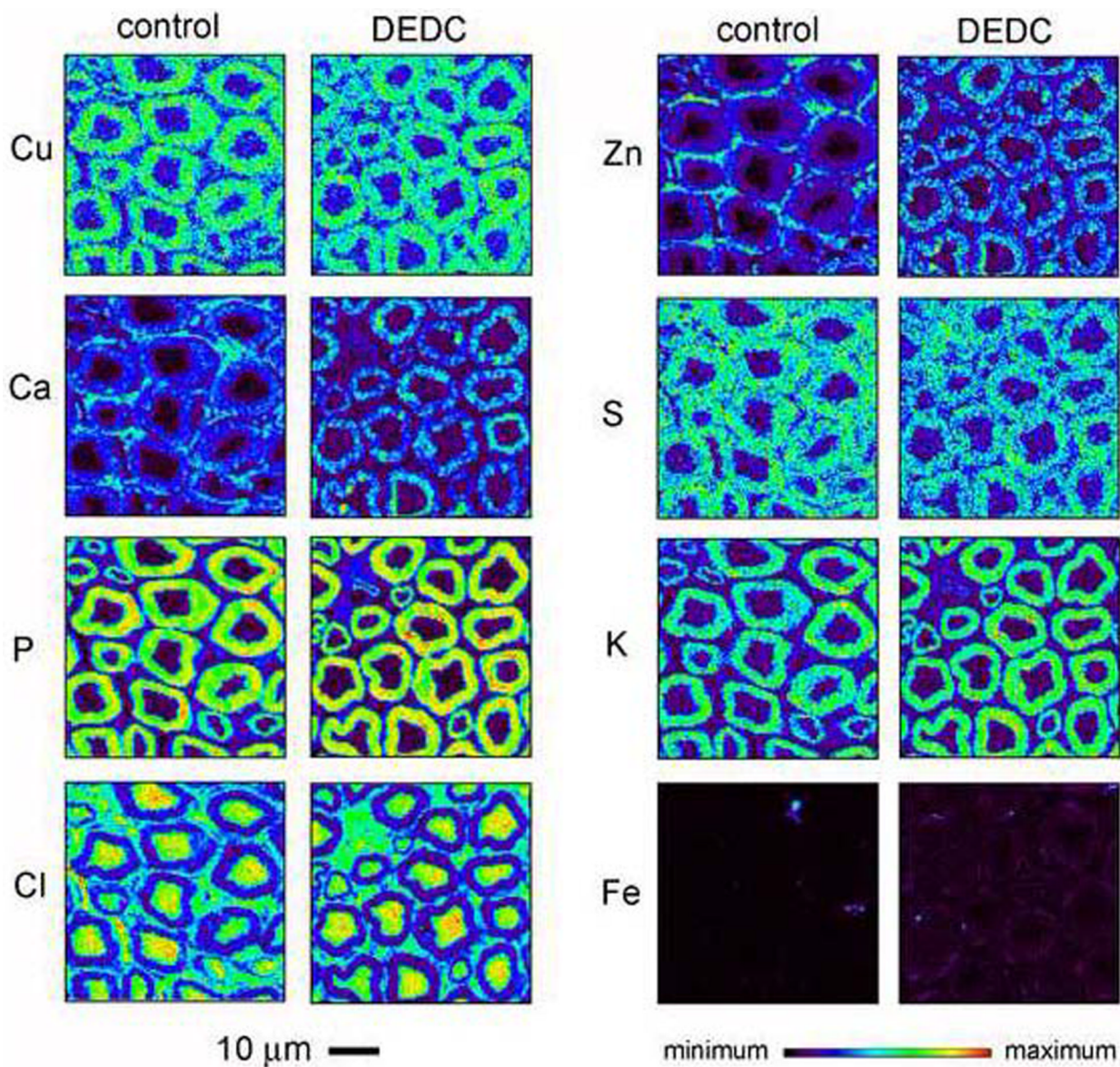
Use of the Advanced Photon Source at Argonne National Laboratory was supported by the U. S. Department of Energy, Office of Science, Office of Basic Energy Sciences, under Contract No. DE-AC02-06CH11357. Experiments were supported in part through the use of the VUMC Research Resource (sponsored by NIH Grants DK20539 and DK58404) and the Vanderbilt University Institute of Imaging Science. This study was supported by NIEHS Grant ES06387 and HIH Grant EB001744. The study sponsors did not contribute to; study design or in the collection, analysis or interpretation of data; in writing of the report; or in the decision to submit the work for publication.

Bibliography

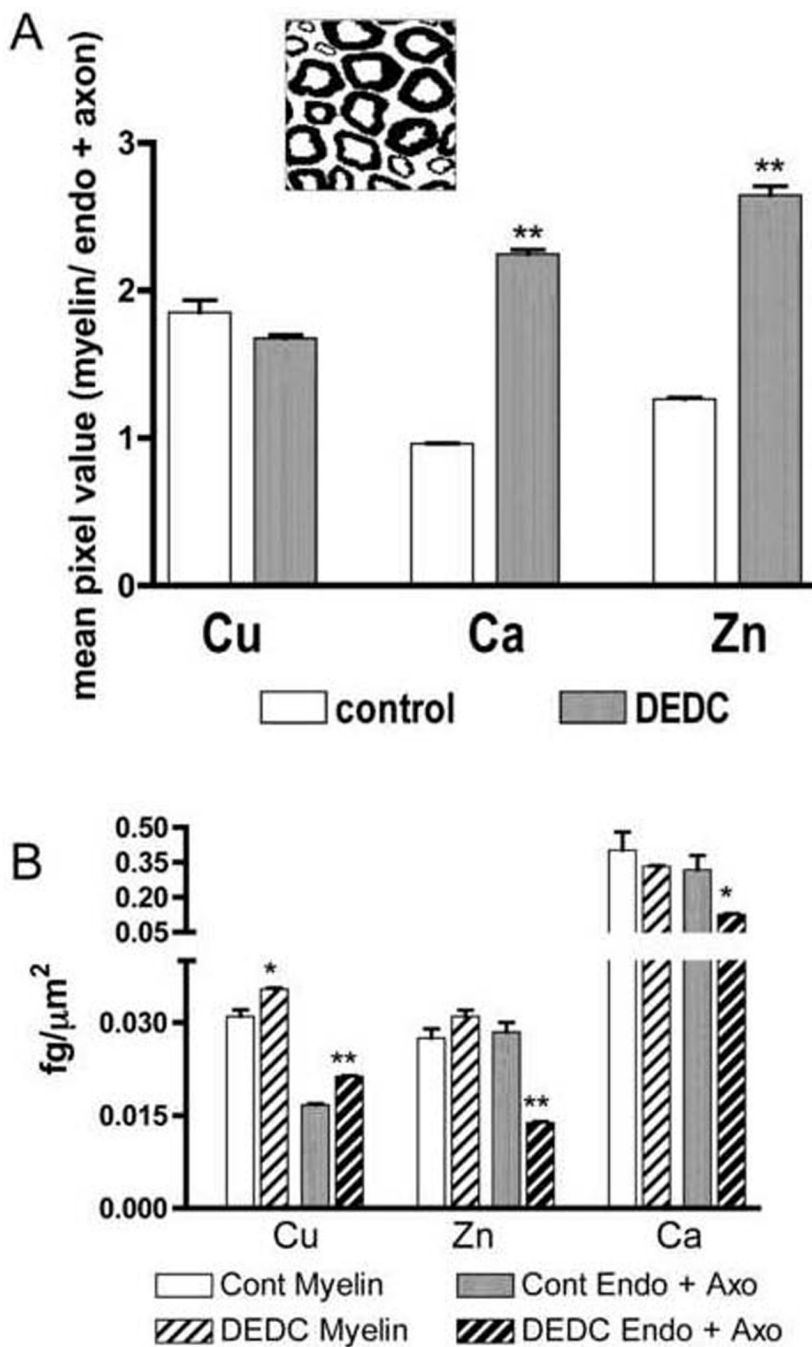
- Awasthi YC, Ansari GA, Awasthi S. Regulation of 4-hydroxynonenal mediated signaling by glutathione S-transferases. *Methods Enzymol* 2005;401:379–407. [PubMed: 16399399]
- Beaulieu C, Fenrich FR, Allen PS. Multicomponent water proton transverse relaxation and T2-discriminated water diffusion in myelinated and nonmyelinated nerve. *Magn Reson Imaging* 1998;16:1201–1210. [PubMed: 9858277]
- Bendszus M, Wessig C, Solymosi L, Reiners K, Koltzenburg M. MRI of peripheral nerve degeneration and regeneration: correlation with electrophysiology and histology. *Exp Neurol* 2004;188:171–177. [PubMed: 15191813]
- Brewer GJ. The risks of free copper in the body and the development of useful anticopper drugs. *Curr Opin Clin Nutr Metab Care* 2008;11:727–732. [PubMed: 18827576]
- Cai Z, Lai B, Yun W, Ilinski P, Legnini D, Maser J, Rodrigues W. A Hard X-Ray Scanning Microprobe for Fluorescence Imaging and Microdiffraction at the Advanced Photon Source. *Am Inst of Physics Conf Proc* 2000;507:472–477.
- Calviello G, Filippi GM, Toesca A, Palozza P, Maggiano N, Nicuolo FD, Serini S, Azzena GB, Galeotti T. Repeated exposure to pyrrolidine-dithiocarbamate induces peripheral nerve alterations in rats. *Toxicol Lett* 2005;158:61–71. [PubMed: 15993744]
- Carmona A, Cloetens P, Deves G, Bohicde S, Ortega R. Nano-imaging of trace metals by synchrotron X-ray fluorescence into dopaminergic single cells and neurite-like processes. *J Anal At Spectrom* 2008;23:1083–1088.
- Chen D, Cui QC, Yang H, Dou QP. Disulfiram, a clinically used anti-alcoholism drug and copper-binding agent, induces apoptotic cell death in breast cancer cultures and xenografts via inhibition of the proteasome activity. *Cancer Res* 2006;66:10425–10433. [PubMed: 17079463]
- Chen SH, Liu SH, Liang YC, Lin JK, Lin-Shiau SY. Death signaling pathway induced by pyrrolidine dithiocarbamate-Cu(2+) complex in the cultured rat cortical astrocytes. *GLIA* 2000;31:249–261. [PubMed: 10941151]
- Chwiej J, Szczerbowska-Boruchowska M, Wojcik S, Lankosz M, Chlebda M, Adamekb D, Tomikb B, Setkowicz Z, Falkenberg G, Stegowski Z, Szczudlik A. Implementation of X-ray fluorescence microscopy for investigation of elemental abnormalities in central nervous system tissue. *J Alloys and Compounds* 2005:401.
- Daniel KG, Chen D, Orlu S, Cui QC, Miller FR, Dou QP. Clioquinol and pyrrolidine dithiocarbamate complex with copper to form proteasome inhibitors and apoptosis inducers in human breast cancer cells. *Breast Cancer Res* 2005;7:R897–908. [PubMed: 16280039]
- Desai V, Kaler SG. Role of copper in human neurological disorders. *Am J Clin Nutr* 2008;88:855S–858S. [PubMed: 18779308]
- Does MD, Snyder RE. Multiexponential T2 relaxation in degenerating peripheral nerve. *Magn Reson Med* 1996;35:207–213. [PubMed: 8622585]

- Fahrni CJ. Biological applications of X-ray fluorescence microscopy: exploring the subcellular topography and speciation of transition metals. *Curr Opin Chem Biol* 2007;11:121–127. [PubMed: 17353139]
- Frisoni GB, Di Monda V. Disulfiram neuropathy: A review (1971-1988) and report of a case. *Alcohol Alcohol* 1989;24:429–437. [PubMed: 2554935]
- Heikkila RE, Cabbat FS, Cohen G. In vivo inhibition of superoxide dismutase in mice by diethyldithiocarbamate. *J Biol Chem* 1976;251:2182–2185. [PubMed: 5443]
- Johnson DJ, Graham DG, Amarnath V, Amarnath K, Valentine WM. Release of carbon disulfide is a contributing mechanism in the axonopathy produced by N,N-diethyldithiocarbamate. *Toxicol Appl Pharmacol* 1998;148:288–296. [PubMed: 9473537]
- King, R. Atlas of Peripheral Nerve Pathology. Oxford University Press Inc.; London: 1999.
- Levine RL, Garland D, Oliver CN, Amici A, Climent I, Lenz AG, Ahn BW, Shaltiel S, Stadtman ER. Determination of carbonyl content in oxidatively modified proteins. *Methods Enzymol* 1990;186:464–478. [PubMed: 1978225]
- Menon RS, Rusinko MS, Allen PS. Proton relaxation studies of water compartmentalization in a model neurological system. *Magn Reson Med* 1992;28:264–274. [PubMed: 1281258]
- Nguyen T, Sherratt PJ, Pickett CB. Regulatory mechanisms controlling gene expression mediated by the antioxidant response element. *Annu Rev Pharmacol Toxicol* 2003;43:233–260. [PubMed: 12359864]
- Nobel CI, Kimland M, Lind B, Orrenius S, Slater AF. Dithiocarbamates induce apoptosis in thymocytes by raising the intracellular level of redox-active copper. *J Biol Chem* 1995;270:26202–26208. [PubMed: 7592825]
- Paunesku T, Vogt S, Maser J, Lai B, Woloschak G. X-ray fluorescence microprobe imaging in biology and medicine. *J Cell Biochem* 2006;99:1489–1502. [PubMed: 17006954]
- Ramagli LS. Quantifying protein in 2-D PAGE solubilization buffers. *Methods Mol Biol* 1999;112:99–103. [PubMed: 10027233]
- Rubinsztein DC. The roles of intracellular protein-degradation pathways in neurodegeneration. *Nature* 2006;443:780–786. [PubMed: 17051204]
- Sabour AA, Sarri-Sarraf N, Saidian S. Thermodynamics of binding copper ion by myelin basic protein. *Thermochimica Acta* 2002;10:147–151.
- Sedzik J, Kotake Y, Uyemura K. Purification of P0 myelin glycoprotein by a Cu²⁺-immobilized metal affinity chromatography. *Neurochem Res* 1999;24:723–732. [PubMed: 10447455]
- Tonkin EG, Erve JC, Valentine WM. Disulfiram produces a non-carbon disulfide-dependent schwannopathy in the rat. *J Neuropathol Exp Neurol* 2000;59:786–797. [PubMed: 11005259]
- Tonkin EG, Valentine HL, Milatovic DM, Valentine WM. N,N-diethyldithiocarbamate produces copper accumulation, lipid peroxidation, and myelin injury in rat peripheral nerve. *Toxicol Sci* 2004;81:160–171. [PubMed: 15187237]
- Tonkin EG, Valentine HL, Zimmerman LJ, Valentine WM. Parenteral N,N-diethyldithiocarbamate produces segmental demyelination in the rat that is not dependent on cysteine carbamylation. *Toxicol Appl Pharmacol* 2003;189:139–150. [PubMed: 12781632]
- Valentine HL, Viquez OM, Amarnath K, Amarnath V, Zyskowski J, Kassa EN, Valentine WM. Nitrogen Substituent Polarity Influences Dithiocarbamate-Mediated Lipid Oxidation, Nerve Copper Accumulation, and Myelin Injury. *Chem Res Toxicol* 2009;22:218–226. [PubMed: 19093748]
- Valentine WM, Amarnath V, Amarnath K, Erve JCL, Graham DG, Morgan DL, Sills RC. Covalent modification of hemoglobin by carbon disulfide: a potential biomarker of effect. *Neurotoxicology* 1998;19:99–108. [PubMed: 9498226]
- Vasilescu V, Katona E, Simplaceanu V, Demco D. Water compartments in the myelinated nerve. III. Pulsed NMR results. *Experientia* 1978;34:1443–1444. [PubMed: 309823]
- Viquez OM, Valentine HL, Amarnath K, Milatovic D, Valentine WM. Copper accumulation and lipid oxidation precede inflammation and myelin lesions in N,N-diethyldithiocarbamate peripheral myelinopathy. *Toxicol Appl Pharmacol* 2008;229:77–85. [PubMed: 18284930]
- Viquez OM, Valentine HL, Friedman DB, Olson SJ, Valentine WM. Peripheral nerve protein expression and carbonyl content in N,N-diethyldithiocarbamate myelinopathy. *Chem Res Toxicol* 2007;20:370–379. [PubMed: 17323979]

- Vogt S. MAPS: A set of software tools for analysis and visualization of 3D X-ray fluorescence data sets. *J. Phys. IV* 2003;104:635–638.
- Webb S, Munro CA, Midha R, Stanisz GJ. Is multicomponent T2 a good measure of myelin content in peripheral nerve? *Magn Reson Med* 2003;49:638–645. [PubMed: 12652534]
- Whittall KP, MacKay AL. Quantitative interpretation of NMR relaxation data. *J. Magn. Reson* 1989;84:134–152.
- Yu Z, Wang F, Milacic V, Li X, Cui QC, Zhang B, Yan B, Dou QP. Evaluation of copper-dependent proteasome-inhibitory and apoptosis-inducing activities of novel pyrrolidine dithiocarbamate analogues. *Int J Mol Med* 2007;20:919–925. [PubMed: 17982703]
- Yun W, Lai B, Cai Z, Maser J, Legnini D, Gluskin E, Chen Z, Krasnoperova A,Y,V, Cerrina F, Di Fabrizio E, Gentili M. Nanometer Focusing of Hard X-Rays by Phase Zone Plates. *Rev Sci Instrum* 1999;70:2238–2241.

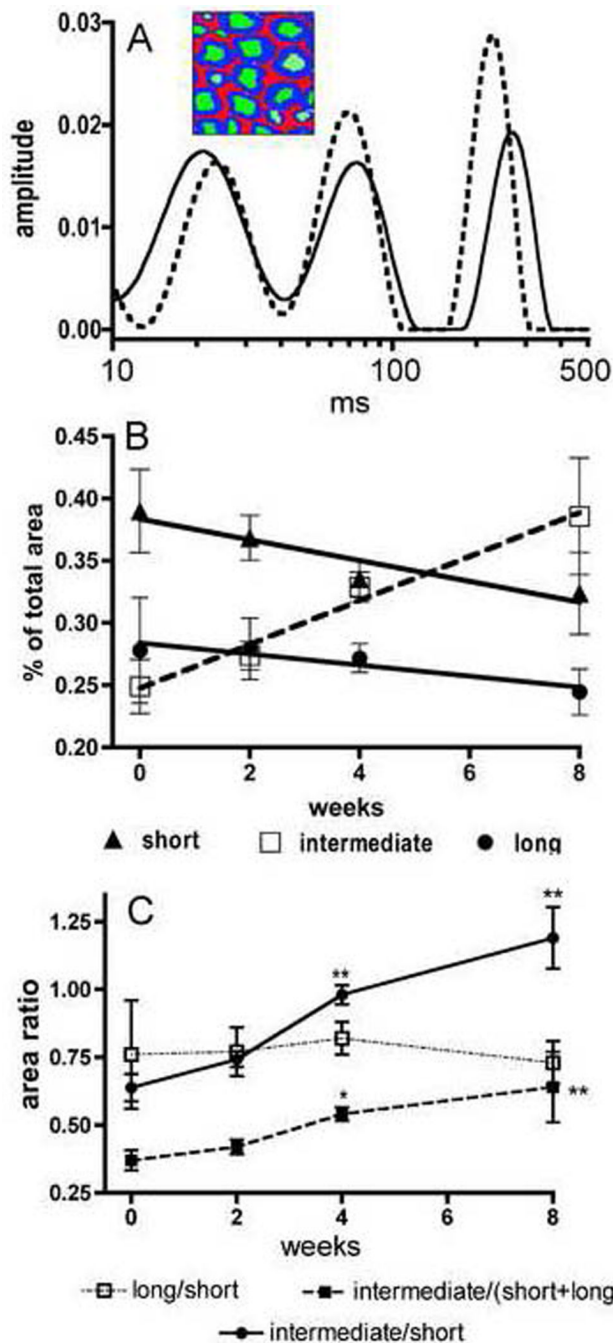


1. Representative two-dimensional elemental maps of sciatic nerve cross-sections from control and DEDC exposed rats generated using synchrotron X-ray fluorescence microscopy. The magnification scale and the LUT scale for element concentrations of all sections are shown at the bottom of the figure.



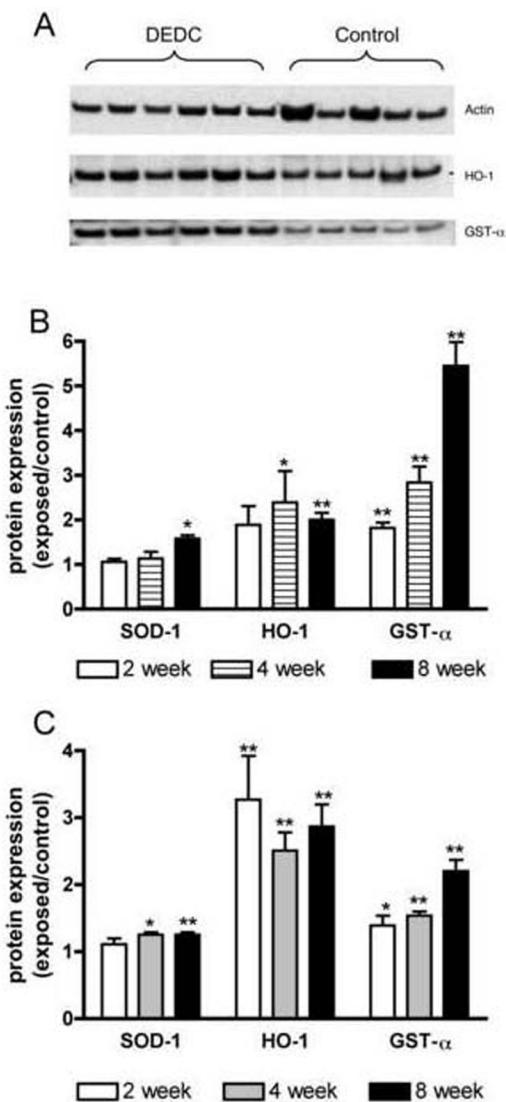
2. Distributions of Cu, Ca, and Zn in sciatic nerve within the myelin, endoneurial (Endo) and axoplasm (Axo) compartments for controls and N,N-diethyldithiocarbamate (DEDC) exposed groups determined by micro-XRF. (A) Ratios of mean element levels in myelin relative to element levels in the endoneurium and axoplasm showing a significant increase for Ca and Zn. ** $p < 0.01$ as determined by one-tailed unpaired student's t-test ($n=2$). The inset shows a representative image segmented into myelin (black) and the endoneurial and axoplasm compartments (white). (B) Mean element concentrations determined for each compartment showed significant increases in both segmented regions for Cu and significant decreases in the

endoneurial and axoplasm compartments for Zn and Ca. $**p < 0.01$ and $*p < 0.05$ as determined by one-tailed unpaired students t-test.

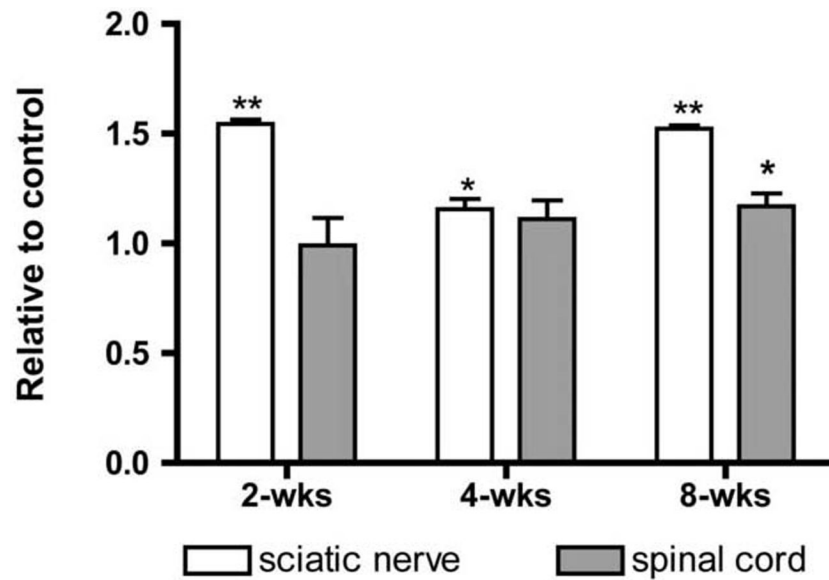


3. Multi-exponential transverse relaxation (MET₂) analyses of sciatic nerve showing the relative quantities of protons within three water pools as a function of dithiocarbamate exposure duration. (A) Two representative spectra of sciatic nerve water T₂ relaxation times are shown illustrating three peaks corresponding to three pools of water protons. The inset illustrates the myelin (blue), axoplasm (green), and extra-cellular (red) water pools attributed to these three relaxation components. The spectrum obtained from a 4 week DEDC exposed animal (dotted line) presents a relative decrease in the contribution to total peak area for the short T₂ component relative to that observed in the control spectrum (solid line). (B) Changes in the contribution of each T₂ relaxation component are shown as a function of DEDC exposure. All

three components demonstrated significant correlations to exposure duration (short component $p < 0.05$, $r^2 = 0.89$; long component $p < 0.05$, $r^2 = 0.87$; and intermediate component $p < 0.01$, $r^2 = 0.98$ as determined by the Pearson correlation test $n=4$). The intermediate component contribution was positively correlated and the short and long components' contributions negatively correlated with increasing exposure duration. (C) The ratios of individual component contribution to total peak area as a function of exposure duration are shown. The ratios of the intermediate component/short component and the intermediate component/(short + long) components increased with longer exposure and were significantly elevated relative to controls at the 4 and 8 week time points (* $p < 0.05$ and ** $p < 0.01$ by one-way ANOVA and Dunnett's post hoc test $n=4$).

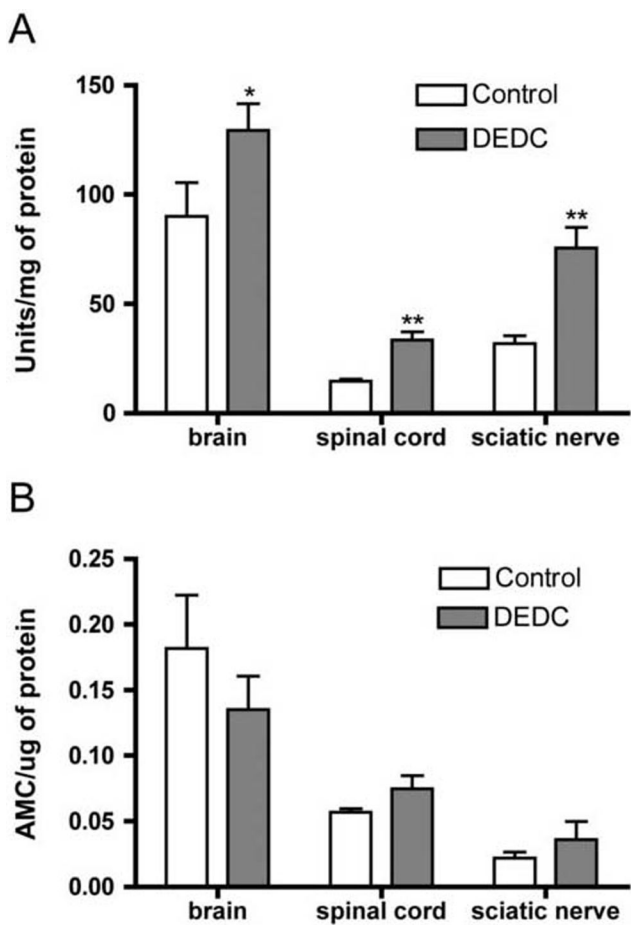


4. Protein expression levels of super oxide dismutase 1 (SOD-1), heme oxygenase-1 (HO-1) and glutathione transferase alpha (GST-α) in controls and rats exposed to N,N-diethyldithiocarbamate (DEDC) for 2, 4 and 8 weeks. (A) Representative western blot showing relative amounts of GST-α, HO-1 and actin proteins isolated from sciatic nerves of control and 8 week DEDC exposed rats. (B) Ratios of exposed to control sciatic nerve SOD-1, HO-1 and GST-α protein levels ((exposed value/actin)/(control value/actin) with n=4 except for the 8 week group where n=6). Error bars represent SE and *p < 0.05 and **p < 0.01 relative to time matched controls determined by unpaired one tailed student's t-test. (C) Ratios of exposed to control spinal cord protein levels of SOD-1, HO-1 and GST-α ((exposed value/actin)/(control value/actin) with n=4 except for the 8 week group where n=6). Error bars represent SE and *p < 0.05 and **p < 0.01 relative to time matched controls determined by unpaired one tailed student's t-test.



5.

Ratios of the total protein carbonyl levels in proteins isolated from sciatic nerves and spinal cords of N,N-diethylthiocarbamate (DEDC) exposed rats to carbonyls in protein obtained from time matched controls determined by slot blot analysis. Isolated proteins from exposed and control rats were derivatized with fluoresceinamine, slot blotted to PVDF membranes, and the amount of protein and protein carbonyls (nmol/mg protein) determined by protein staining with densitometry and immunodetection with chemiluminescence, respectively (see Materials and Methods for details). Levels of protein carbonyls in samples from exposed animals are presented relative to those obtained for time-matched controls. In sciatic nerve samples significant increases were observed at all time points examined and for spinal cord in the 8 week exposure group. (* $p < 0.05$ and ** $p < 0.01$ by unpaired one-tailed student's t-test, $n = 4$ except for the 8 week groups where $n = 5$ for controls and $n = 6$ for DEDC exposed)



6. Superoxide dismutase 1 (SOD-1) and proteasome activity in brain, spinal cord and sciatic nerve of controls and rats exposed to N,N-diethyldithiocarbamate (DEDC) for 8 weeks. (A) SOD-1 activity determined as units/mg protein based upon the autoxidation of 5,6,6a,11b-tetrahydro-3,9,10 trihydroxybenzo[c]fluorine following inactivation of SOD-2 (see Materials and Methods for details) (* $p < 0.05$ and ** $p < 0.01$ relative to control by unpaired one-tailed student's t-test $n = 5$ for controls and $n = 6$ for DEDC exposed). (B) Proteasome activity determined from the generation of free amino-4-methylcoumarin (AMC) from an LLVY-AMC substrate. No significant differences were detected.

Table 1^aSciatic nerve element levels determined by micro-XRF

Element	Control	DEDC	^b p value
Zn	27.7 (3.4)	22.5 (0.5)	.08
Cu	23.8 (1.9)	28.7 (0.3)	.03
Ca	360.0 (115.9)	231.0 (1.1)	.12
S	1236.9 (114.4)	1346.3 (79.1)	.19
P	40622 (4257)	36825 (21.4)	.17
K	276.9 (72.4)	346.7 (51.5)	.19
Cl	13667.3 (889.8)	15839.9 (516.7)	.05
Fe	29.7 (1.8)	27.2 (0.7)	.11

^aTotal elemental levels (mean pixel value × scan area) in fg per section (SD) determined by x-ray fluorescence microscopy (n = 2)

^bdetermined by one-way unpaired students t-test